

(will be inserted by hand later)

Your thesaurus codes are:

08.01.1; 08.05.03; 10.15.2

ASTRONOMY  
AND  
ASTROPHYSICS  
3.1.1997

NASA-CR-204768

## Lithium abundances in the young open cluster IC 2602\*

S. Randich<sup>1</sup>, N. Aharpour<sup>2</sup>, R. Pallavicini<sup>3</sup>, C.F. Prosser<sup>4</sup>, and J.R. Stauffer<sup>4</sup><sup>1</sup> European Southern Observatory, Karl-Schwarzschild-Straße 2, D-85748 Garching bei München, Germany<sup>2</sup> Dipartimento Astronomia, Università di Firenze, Largo Fermi 5, I-50125 Firenze, Italy<sup>3</sup> Osservatorio Astronomico di Palermo, Piazza del Parlamento 1, I-90134, Palermo, Italy<sup>4</sup> Harvard -Smithsonian Center for Astrophysics, 60 Garden St. MS-66 Cambridge, MA 02138

Received date; accepted date

032503

**Abstract.** We have obtained high-resolution spectra for 28 candidate late-type stars in the 30 Myr old cluster IC 2602. NLTE Li abundances have been derived from measured equivalent widths. The  $\log n(\text{Li}) - T_{\text{eff}}$  and  $\log n(\text{Li}) - \text{mass}$  distributions for our sample stars have been compared with those of the Pleiades and  $\alpha$  Persei. Our data show that F stars in the three clusters have the same lithium content, which corresponds to the initial content for Pop. I stars. G and early-K IC 2602 stars are, on average, somewhat more Li-rich than their counterparts in the two slightly older clusters. Finally, the latest-type IC 2602 stars are heavily Li depleted, with their Li content being as low as the lowest measured among the Pleiades. As in the Pleiades and  $\alpha$  Per, a star-to-star scatter in lithium is observed among 30 Myr old late-K/early-K dwarfs in IC 2602, indicating that this spread develops in the pre-main sequence phases.

**Key words:** Stars: abundances, stars: evolution, open clusters and association: individual(IC 2602)

temperature, or mass, and stellar age, with convection being possibly the main Li depletion mechanism. However, although the scenario of a declining Li abundance with increasing age and spectral type is valid in a statistical sense, several contradictory observational results were found. Particularly, as far as young open clusters are concerned (age  $< 10^9$  years), two major puzzling and controversial points stand out. Namely, *i*) the presence of the 'dip' -or a steep decrease of  $\log n(\text{Li})$  within a narrow 300 K interval around 6600 K, which is observed in clusters older than  $\sim 1 \times 10^8$  years (see Balachandran 1995 and references therein); *ii*) the dispersion in Li at a given spectral type, which is observed among late-type stars in the 50 Myr old  $\alpha$  Per and 70 Myr old Pleiades clusters (e.g., Balachandran et al. 1988; García Lopez et al. 1991, 1994; Soderblom et al. 1993a; Soderblom 1995 and references therein). Since in the present paper we focus on the early main sequence evolution of Li, we will not discuss the 'dip' problem; nevertheless, we would like to stress that the above problems both indicate that convection is not the only mechanism affecting Li abundance and that the evolution of Li is not determined solely by three parameters (i.e., age, mass, and metallicity), but additional ones are needed in order to describe and understand it (see also Pasquini et al. 1994, 1997). It is indeed commonly accepted now that additional parameters such as rotation, play a role in Li destruction or preservation.

## 1. Introduction

Several studies have been carried over the past 15 years, addressing the time evolution of lithium abundance among Pop. I stars by means of observations of open clusters of different ages (e.g., Duncan & Jones 1983; Boesgaard & Tripicco 1986; Butler et al. 1987; Balachandran et al. 1988; Boesgaard et al. 1988; Soderblom et al. 1990; Michaud & Charbonneau 1991; Thorburn et al. 1993; Soderblom et al. 1993a; Balachandran 1995). These investigations, complemented by surveys of Li in field stars, have indicated that, at a given metallicity, Li surface abundance in late-type stars is a decreasing function of both effective

Duncan & Jones (1983) first pointed out the existence of a scatter in Li among late-G and K Pleiades stars at the same color. Subsequent studies confirmed that a spread in lithium is present among Pleiades dwarfs with  $(B-V)_0 \geq 0.75$  (or  $M \leq 0.9 M_{\odot}$ ) as well as in  $\alpha$  Persei late-type stars (Balachandran et al. 1988). On the contrary, high resolution, high signal to noise spectra of a dozen Hyades K dwarfs suggest that this  $\sim 600$  Myr old cluster lacks the spread in Li, or, if present, it is much less than that measured in the Pleiades (Soderblom et al. 1995). Balachandran et al. (1988) also reported the existence of a few 'weak-Li' objects in  $\alpha$  Per having a Li content lower

Send offprint requests to: S. Randich, e-mail: [srandich@eso.org](mailto:srandich@eso.org)

\* Based on observations collected at ESO, La Silla

than what was measured in the older Hyades stars at the same color; however, reanalysis of the data has shown that this result was spurious and that these stars have Li abundances consistent with those of the other cluster members (Balachandran et al. 1996). Li abundances appear to be correlated with rotation for late-G and early-K dwarfs, in the sense that stars which rotate more rapidly also show generally higher Li abundances (Butler et al. 1987; Soderblom et al. 1993a); this Li- $v_{\text{sin}i}$  relationship breaks down for stars cooler than  $T_{\text{eff}} \sim 4400$  K (García Lopez et al. 1994; Soderblom et al. 1995). Soderblom et al. (1993a) have ruled out the hypothesis that chromospheric activity (through the presence of cool spots, or variations in the line formation conditions) could be responsible for the apparent spread in Li. They also excluded, or regarded as very unlikely, other effects such as a spread in age, different initial abundances, autogenesis, accretion of new Li-rich material, and mass loss. Rotation was regarded as the most likely additional parameter affecting the evolution of Li, at least in the  $0.7 - 0.9 M_{\odot}$  range, causing the observed dispersion in Li abundances. The detailed mechanism, though, is still elusive and, as Soderblom et al. noted, theoretical models have not been able up to now to fully/quantitatively match the observational results. The conclusive remark in Soderblom et al.'s paper can be used as an introductory remark to the present paper: *“Going to even younger clusters will show when and how the spread in  $N_{\text{Li}}$  develops—those are surely valuable clues to the mechanism”*.

We present here a Li survey in the IC 2602 open cluster. IC 2602, with an estimated age of 30 Myr (Stauffer et al. 1997), provides a good opportunity to fill the age gap between pre-main sequence (PMS) and early main sequence stars in the empirical study of Li abundance. In other words, we hope with the present study to better constrain the early evolution of Li abundance and to understand whether the spread develops in the last phases of approach towards the main sequence or during the early phases on the main sequence. At 30 Myr, the G stars of IC 2602 have just arrived on the Zero Age Main Sequence (ZAMS), while later-type objects are still evolving to the ZAMS. Their Li content therefore should be the result of PMS processes only.

## 2. Data sample and observations

### 2.1. Data sample

IC 2602 has been poorly studied up to now: while some photometric and spectroscopic studies had been carried out for high-mass (spectral types earlier than F5) cluster members (e.g., Whiteoak 1961; Braes 1962), basically no information was available so far for solar-type and low mass stars. ROSAT PSPC observations of the cluster together with two CCD photometric surveys have enabled Randich et al. (1995) and Prosser et al. (1996) to create a

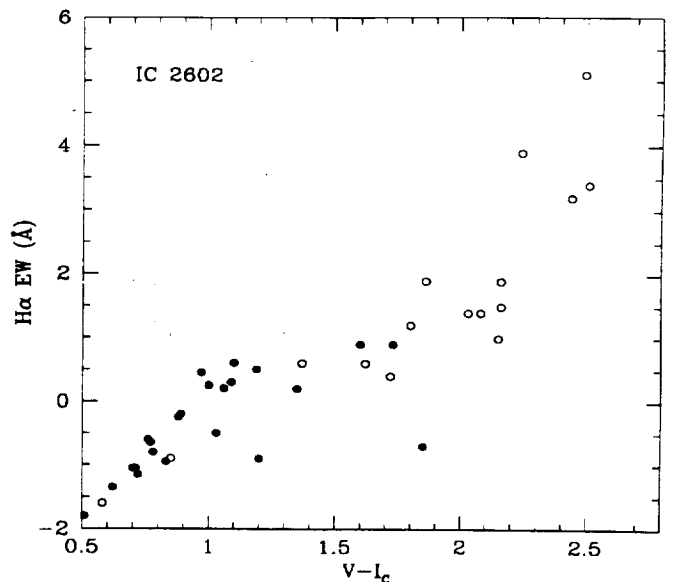


Fig. 1.  $H_{\alpha}$  EW as a function of  $V-I_C$  color for IC 2602 stars observed by Stauffer et al. (1996). The objects included in our sample are represented by filled circles.

preliminary list of low mass members of the cluster. The combined CCD and X-ray surveys yielded a total of 69 new probable or possible cluster members. However, both the photometric and the X-ray selection suffer from contamination from field stars (see discussion in Randich et al. 1995) and thus cluster membership for these objects has to be confirmed by additional indicators, radial velocity in the first place. One of the aims of our follow-up high resolution observations was indeed to confirm the membership status of these cluster candidates.

In the present paper we report the results of high resolution spectroscopic observations of 28 objects, 18 of which are new cluster candidates from the X-ray/photometric surveys, while the remaining 10 are previously known cluster members. The observed stars are listed in Table 1, where we give the running ‘R’ identification number from Randich et al. (1995) and, when available, the ‘B’ or ‘W’ ID’s from the Braes and Whiteoak catalogs, or the GSC number. Spectral types, if available, are listed in column 3. Photometric data, specifically V magnitudes, B-V and V- $I_C$  colors, are given in columns 4, 5 and 6. A membership flag based on photometry is given in column 7; such a flag was assigned following the same selection criterion as in Randich et al. (1995) and Prosser et al. (1996): objects within  $\sim 1$  mag above and  $\sim 0.3$  mag below the 30 Myr single star isochrone in both the V vs. B-V and V vs. V- $I_C$  diagrams were considered good photometric candidates (‘Y’), whereas objects located at the border or slightly outside the above limits in either diagram, were considered as uncertain candidates (‘?’). A membership flag based on radial velocities is then given in column 8

Table 1. The observed sample

R	Other	Sp. <sup>a</sup>	V <sup>b</sup>	B-V <sup>b</sup>	V-I <sub>C</sub> <sup>b</sup>	phot. Mem.	v rad Mem	v sin i	H $\alpha$ E.W. <sup>c</sup>	notes
3	GSC8964.0165		11.32 (5)	0.87 (5)	0.89 (5)	Y	?	25	-0.2	SB1?
7	GSC8960.1942		9.21 (5)	0.44 (5)	0.46 (5)	Y	?	52	-1.5	SB1?
14	GSC8964.0606		11.57 (5)	0.87 (5)	0.88 (5)	Y	Y	13	-0.25	
15	GSC8964.0073		11.75 (5)	0.93 (5)	1.06 (5)	Y	Y	10	+0.2	
18	GSC8964.0853		12.49 (5)	1.05 (5)	1.20 (5)	Y	Y	11	-0.9	
21	B6=HD91895	G0	9.50 (4)	0.51 (4)	0.62 (4)	Y	Y	23	-1.35	
29	GSC8965.1524		12.73 (6)	1.11 (5)	1.19 (4)	Y	Y	22	+0.5	
35	W71	G5	10.59 (4)	0.40** (1)	0.70 (4)	Y	Y	20	-1.05	
43	GSC8965.0238		12.14 (6)	0.95 (6)	1.10 (6)	Y	Y	50	+0.6	
45	GSC8961.0383		10.73 (5)	0.66 (5)	0.72 (5)	Y	Y	23	-1.15	
49	GSC8965.0162		11.71 (4)	0.75 (4)	0.94 (4)	Y	N	$\leq 10$	-1.2	
53A			14.04 (6)	1.89 (5)	1.85 (4)	N	?	10	-0.7	
56			13.64 (6)	1.43 (5)	1.59 (4)	Y	Y	17	+0.9	
58	B102=HD307938	G0	10.52 (5)	0.65 (5)	0.74 (5)	Y	Y	93	-0.65	
59	GSC8965.0231		11.86 (4)	0.82 (4)	1.00 (4)	Y	Y	34	+0.25	
66	GSC8965.0432		11.07 (4)	0.68 (4)	0.83 (4)	Y	Y	10	-0.95	
68	W84=HD307960	G5	11.23 (5)	0.86 (5)	1.09 (4)	Y	Y	48	+0.3	
70	W85=HD307936	F7	10.91 (4)	0.69 (4)	0.71 (4)	Y	Y	10	-1.05	
72	B120=HD307979	G0	10.89 (5)	0.64 (5)	0.76 (5)	Y	Y	49	-0.6	
73B	GSC8965.0084		11.06 (4)	...	1.29 (4)	?	N	$\leq 10$	-1.15	
79	B44=HD93405	F2V	9.08 (4)	0.44 (2)	0.51 (4)	Y	Y	57	-1.8	
80	B134=HD308016	G5	10.60 (3)	0.95 (3)	1.00 (3)	?	?	10	-0.5	
83	GSC8965.0308		10.70 (4)	0.62 (4)	0.78 (4)	Y	Y	30	-0.8	
85	B131=HD308012	F8	9.87 (4)	0.52 (4)	0.58 (4)	Y	Y	45	-1.5	
89			12.97 (6)	1.24 (5)	1.35 (4)	Y	Y	14	+0.2	
92	B132=HD308013	G	10.28 (4)	0.69 (3)	0.78 (4)	Y	Y	14	-0.8	
94			13.33 (6)	1.39 (5)	1.73 (4)	Y	Y	23	+0.9	
95A	GSC8965.1276		11.73 (6)	0.87 (5)	0.97 (4)	Y	Y	12	+0.45	

a: Spectral types from Abt & Morgan (1972), Whiteoak (1961), or HD spectral type listed in Braes (1962).

b: Source for photometry:

- (1): Whiteoak (1961), photographic
- (2): Whiteoak (1961), photoelectric
- (3): CTIO photoelectric photometry
- (4): '92/'93 CCD survey
- (5): '95 CCD survey
- (6): average of '92/'93 and '95 CCD surveys

c: from Stauffer et al. (1996)

\*: B-V for R35 comes from Whiteoak's (1961) photographic photometry and is likely in error.

We have derived B-V for R35 from its V-I<sub>C</sub> by fitting the relationship for the other cluster candidates, obtaining B-V=0.67

of Tab. 1: whereas 'Y' or 'N' indicate that vrad is clearly consistent or inconsistent with cluster membership, there are four uncertain cases which were indicated with a '?'. In these cases, radial velocities are slightly off the mean value for the cluster, but the differences are within the errors or there are indications for binarity. In columns 9 and 10 we list rotational velocities and H $\alpha$  equivalent widths as derived from our spectra (see Stauffer et al. 1997), while additional notes concerning possible binaries are given in column 11. More detailed results on radial velocities and cluster membership analysis, as well as on chromospheric activity and rotational velocities for the sample stars, have

been presented by Stauffer et al. (1997). Since we intend to focus our study on Li abundances, we have just summarized the information on radial velocities and on H $\alpha$  with the specific aim to single out possible and probable cluster non-members in our observed sample. With the same purpose, we also plot in Figure 1 H $\alpha$  equivalent widths as a function of V-I<sub>C</sub> for the sample of IC 2602 stars of Stauffer et al. (1997), which includes the objects in the present study. The figure shows that the vast majority of stars later than V-I<sub>C</sub>~1 have H $\alpha$  in emission. Tab. 1 shows that R49, R53A, and R73B are definitively non-members, as indicated by their radial velocities and/or

photometry; these objects will be dropped from further analysis/discussion. We retain all of the other stars as possible members for the present. However, we note that R80 is suspect, because both its photometry and radial velocity are somewhat discrepant from average and H $\alpha$  is in absorption when other cluster members of the same color all have H $\alpha$  emission (see Fig. 1).

## 2.2. Observations

The observations were carried out at the European Southern Observatory (ESO) in April '94, using the 3.6 m telescope in conjunction with the Cassegrain Echelle Spectrograph (CASPEC, Pasquini 1993 and references therein). The combination 'standard' echelle grating (31.6 lines mm<sup>-1</sup>), red cross-disperser (158 lines mm<sup>-1</sup>) and short camera (focal length= 291 mm, f/1.46) was used. The above combination, together with ESO CCD #32 (TK512, with 512 $\times$  512 pixels<sup>2</sup> of 27 $\mu$ <sup>2</sup>) and a slit aperture of 280  $\mu$ m (2.1 arcsec on the sky), resulted in a nominal resolving power of R = 20,000 (or a two pixel resolution element  $\Delta\lambda \sim 0.35 \text{ \AA}$  at 6700  $\text{\AA}$ ). A spectral interval of  $\sim 2800 \text{ \AA}$  was covered, ranging from  $\lambda \simeq 5500 \text{ \AA}$  to  $\lambda \simeq 8300 \text{ \AA}$ .

Due to the range in magnitude of our sample stars and to variable weather conditions, the quality of our spectra differs from star to star, with typical S/N ratios ranging between 40 and 80. Data reduction was performed using MIDAS and following the usual steps, i.e. background subtraction, flat-fielding, order extraction, wavelength calibration. Examples of the acquired spectra in the Li and H $\alpha$  order are shown in Figure 2 for three stars of different spectral type.

## 3. Data Analysis

### 3.1. Effective temperatures

One of the aims of the present work is the comparison of IC 2602 with the Pleiades cluster and an analysis as close as possible to the one carried out by Soderblom et al. will help to avoid systematic differences. We therefore determined temperatures from the B-V color employing the scale used by Soderblom et al. (1993a,b) for the Pleiades, which they derived by fitting the temperature/color data of Bessel (1979) in the 4000 - 7000 K range. In inferring  $T_{eff}$  we assumed a reddening  $E(B-V)=0.04$  (e.g., Whiteoak 1961; Braes 1962). As stressed by Soderblom et al., their calibration is in good agreement with those of Arribas & Roger (1989) and Boesgaard and Friel (1990). In order to carry out an additional check on how alternative  $T_{eff}$  vs. B-V calibrations or the use of a different color index might affect our analysis, we derived effective temperatures a) through the calibration used by Thorburn et al. (1993) for the Hyades; b) employing a  $T_{eff}$  vs. V-I<sub>C</sub> scale which we obtained consistently with

Soderblom et al. (1993a,b), i.e., fitting Bessel's (1979) data. The relationship which we found has the form:

$$T_{eff} = 9900 - 8598 (V-I_C)_o + 4246 (V-I_C)_o^2 - 755 (V-I_C)_o^3$$

We found a general good agreement between  $T_{eff}$  derived from Soderblom et al.'s and Thorburn et al.'s calibrations: if we exclude R53A, whose temperature is far beyond the range of validity of Thorburn et al.'s calibration, the differences do not exceed 100-130 K, the average difference being 80 K.  $T_{eff}$ 's derived following Thorburn et al. are always somewhat larger than those from Soderblom et al.'s calibration, implying that by using their temperature scale we would get slightly larger Li abundances. On the contrary, temperatures inferred from V-I<sub>C</sub> are in several cases different from those derived from B-V as shown in Figure 3, where  $T_{eff}$  derived from the two colors are compared. A scatter is also present in the plot, i.e. stars with similar  $T_{eff}$  (B-V) show a range in  $T_{eff}$  (V-I<sub>C</sub>). While there are objects with  $|\Delta T_{eff}|$  of the order of 50 K or lower (with  $|\Delta T_{eff}| = |T_{eff}(V-I_C) - T_{eff}(B-V)|$ ), others have differences of the order of 200 to 400 K; in most cases  $T_{eff}(V-I_C)$  are lower than  $T_{eff}(B-V)$ . A similar effect was pointed out by García Lopez et al. (1994) for their Pleiades and  $\alpha$  Persei samples. Specifically, they found a significant dispersion when comparing temperatures derived from B-V colors with those inferred from either V-I<sub>C</sub> or R-I, and suggested as possible reasons chromospheric activity, rapid rotation, or incorrect reddening estimate, which would affect B-V and V-I<sub>C</sub> in a different way. These causes are probably valid also for IC 2602 stars. While we have assumed a mean reddening of  $E(B-V)=0.04$ , published reddening values range between 0.0 and 0.15 for individual stars (Whiteoak 1961) and thus it is not unlikely that different objects in our sample have a different reddening. As to the effect of activity on colors, the point is controversial. While Soderblom (1989) had showed that the determination of temperature from color indices is not influenced in a major way by color anomalies, Campbell (1984) suggested that chromospheric activity could cause color anomalies among Hyades low mass dwarfs. Along the same line, Stauffer (1984) had shown that there is a spread in the B-V vs V-I<sub>C</sub> diagram for the Pleiades, with the rapid rotators displaced on average about 0.04 mag blueward in B-V (for a given V-I<sub>C</sub>) relative to slow rotators. He advocated that this was due to the fact that rapid rotators would be more covered with spots than slow rotators. Most of the IC 2602 stars in our sample show a high level of X-ray activity and thus it is not unlikely that they are covered with spots and that they have apparent redder V-I<sub>C</sub> colors as suggested also by Stauffer et al. (1997). We also note that photometric variability (possibly affecting B-V and V-I<sub>C</sub> colors differently), due again to spots and rotational modulation, is expected in active stars (e.g., Bouvier 1996), contributing to the uncertainty in the inferred  $T_{eff}$ 's. To conclude, since there is no obvious way to determine which is the

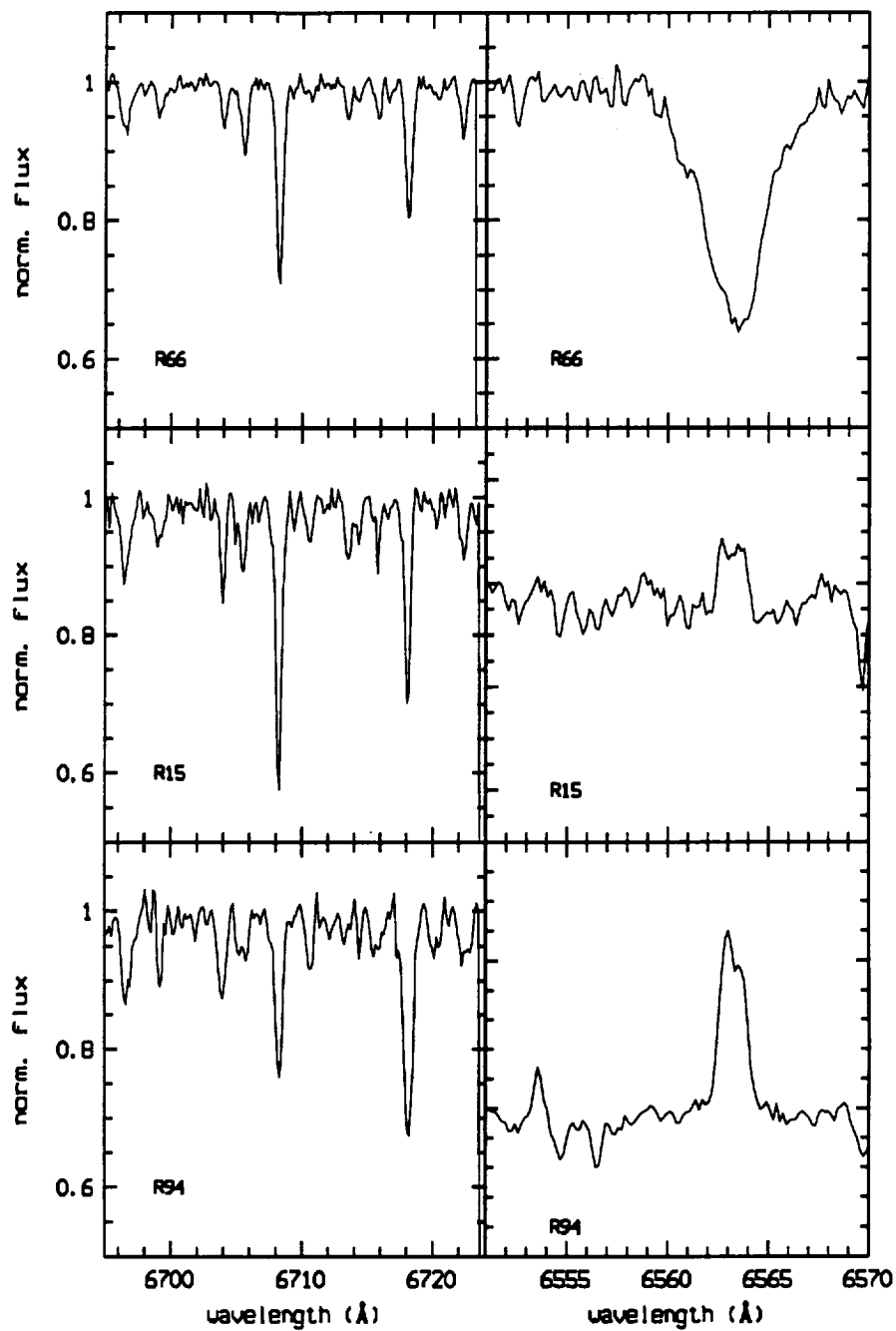


Fig. 2. Examples of the acquired spectra. In the left hand panels we show spectra in the Li region for R94 ( $B-V=1.39$ ), R15 ( $B-V=0.93$ ), and R66 ( $B-V=0.68$ ) (bottom to top). In the right hand panels H $\alpha$  spectra for the same stars are shown.

right temperature, in the following analysis we will use temperatures derived from B–V colors, both for consistency with the Soderblom et al.’s analysis and in order not to get ‘artificially’ cooler temperatures due to the effect of spots.

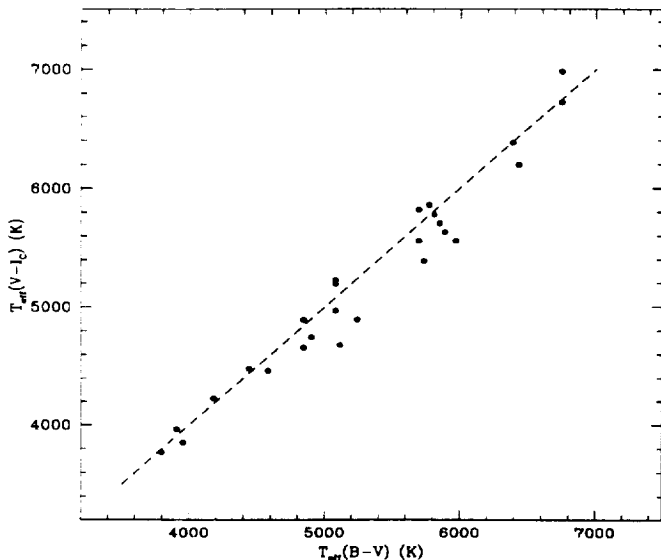


Fig. 3.  $T_{eff}$  from  $V-I_C$  colors vs.  $T_{eff}$  from B–V (see text).

### 3.2. Lithium abundances

The equivalent widths of the 6707.44 Fe I + 6707.81 Li I Å blend and of the 6717.69 Ca I Å feature were measured for ‘Y’ and ‘?’ stars in Tab. 1. The wavelength separation between the 6707.44 Fe I line and the Li feature is only slightly larger than one resolution element, thus the two features are not completely resolved even in the best cases of slowly rotating objects. We corrected for the contribution of the 6707.44 Å feature (which is actually a blend of Fe I and molecular lines) using Soderblom et al.’s (1993a) analytical approximation for the EW of this line as a function of  $(B-V)_o$ :  $EW(6707.44) = 20 \times (B-V)_o - 3$  mÅ. According to Soderblom et al. this relationship is accurate to 3 to 5 mÅ.

The major source of error on the measured equivalent widths comes from the quality of our spectra, due to rapid rotation and/or relatively low S/N. For rapidly rotating stars it is difficult to define the position of the depressed continuum and the Li feature might be blended with other features in addition to the 6707.44 Å line. The comparison of a narrow lined spectrum of a slowly rotating star with the broadened spectrum of a rapid rotator of a similar color allowed us to determine whether other features were contributing to the 6707.8 Å Li blend.

For all but one (R58) of the rapidly rotating objects (i.e.,  $v \sin i > 30$  km/sec), we are confident that the presence of other features should not affect in a significant way the estimated EW of the Li doublet. On the other hand, the comparison of the spectrum of R58 ( $(B-V)_o = 0.65$ ,  $v \sin i = 59$  km/sec) with that of R70 ( $(B-V)_o = 0.69$ ,  $v \sin i = 10$  km/sec) showed that the measured EW of the Li blend for R58 is probably overestimated by 30–40 mÅ. The Li abundance of this object was therefore derived subtracting 35 mÅ from the measured equivalent width. The measured EW’s of the 6707.44 + 6707.81 Å blend and of the Ca 6717.69 Å line are listed in columns 3 and 4 of Table. 2, while in column 5 we list the estimated correction for the contribution of the 6707.44 Å Fe feature. In the first two columns of the table R numbers and inferred temperatures are given. The quoted errors in EW’s represent the rms about the average of several EW measurements which were carried out changing the position of the continuum. The random uncertainty on the measured equivalent widths was also estimated by computing the rms scatter about a mean relationship between the Ca I line equivalent width and  $(B-V)_o$ : this rms was found to be 14.8 mÅ.<sup>1</sup>

Li abundances were determined using Soderblom et al.’s (1993a) LTE curves of growth (COG). We assumed that the parameters they used for the 70 Myr old Pleiades dwarfs (in particular surface gravity and microturbulence velocity<sup>2</sup>) are adequate also for the 30 Myr old dwarfs in IC 2602. Since the COG’s of Soderblom et al. are computed over  $4000 < T_{eff} < 6500$  K, only upper or lower limits to  $\log n(\text{Li})$  were derived for respectively cooler or warmer objects.

The abundance analysis was repeated also using the NLTE code of Carlsson et al. (1994); namely, NLTE corrections to LTE abundances were computed, starting from the LTE abundances themselves. A metal abundance  $[\text{Fe}/\text{H}] = 0$  and a gravity  $\log g = 4.5$  were assumed. Such a  $\log g$  value is appropriate for dwarfs at 30 Myr, in the  $\sim 1.4\text{--}0.7 M_\odot$  mass range, according to the isochrone of Swenson et al. (1994). Carlsson et al.’s code provides NLTE corrections only for objects with  $T_{eff} \geq 4500$  K, and thus NLTE abundances were derived only for objects warmer than this. The results of our analysis are listed in Tab. 2:  $\log n(\text{Li})_{LTE}$  computed using Soderblom et al.’s COG’s are listed in column (6) in the usual logarithmic scale  $\log N(\text{H}) = 12$ , followed by the  $\log n(\text{Li})_{NLTE}$  obtained from NLTE analysis.

<sup>1</sup> In computing the mean relationship and the rms about it, R18 and R53 were excluded from the sample, since their Ca I EW’s are clearly discordant from the trend for the other objects.

<sup>2</sup> In their paper Soderblom et al. do not quote any value for the assumed  $\log g$ , while their curves of growth were computed for a microturbulence  $\xi = 1.0$  km/sec.

Table 2. Lithium Abundances

R	$T_{eff}$ (K)	$W_{\lambda}(\text{Li+Fe})$ (mÅ)	$W_{\lambda}(\text{Ca } 6717.69\text{Å})$ (mÅ)	$W_{\lambda}(\text{Fe}6707.44\text{Å})$ (mÅ)	$n(\text{Li})_{LTE}$	$n(\text{Li})_{NLTE}$
3	5080	265 ± 13	151 ± 5	13.6	2.85	2.74
7	6750	65 ± 17	99 ± 25	5.0	> 2.97	...
14	5080	230 ± 10	177 ± 10	13.6	2.61	2.58
15	4900	259 ± 12	178 ± 10	14.8	2.56	2.55
18	4560	≤ 17	67 ± 6	17.2	≤ -0.57	...
21	6430	119 ± 10	110 ± 5	6.4	3.32	3.18
29	4440	239 ± 11	237 ± 10	18.4	1.76	...
35	5770	215 ± 8	138 ± 9	9.6	3.33	3.12
43	4840	355 ± 20	193 ± 20	15.2	3.17	2.99
45	5810	151 ± 7	124 ± 5	9.4	2.97	2.87
56	3910	138 ± 6	305 ± 20	24.8	≤ 0.65	...
58	5850	234(190) ± 27	108 ± 30	9.2	3.55 (3.31)	3.26 (3.12)
59	5240	305 ± 15	159 ± 10	12.6	3.36	3.09
66	5730	186 ± 6	135 ± 8	9.8	3.10	2.97
68	5110	266 ± 10	170 ± 10	13.4	2.90	2.77
70	5700	168 ± 8	139 ± 5	10.0	2.95	2.85
72	5890	209 ± 15	141 ± 15	9.0	3.41	3.19
79	6750	61 ± 20	50 ± 15	5.0	>2.94	...
80	4840	188 ± 8	223 ± 6	15.2	2.02	2.14
83	5970	203 ± 6	127 ± 10	8.6	3.45	3.22
85	6390	103 ± 10	66 ± 7	6.6	3.17	3.06
89	4180	265 ± 8	260 ± 6	21.0	1.60	...
92	5690	195 ± 10	147 ± 6	10.0	3.12	2.98
94	3950	174 ± 8	313 ± 15	24.0	≤ 0.87	...
95A	5080	317 ± 15	184 ± 7	13.6	3.23	2.99

## 4. Results

### 4.1. Lithium in IC 2602

#### 4.1.1. Equivalent widths

Our results are shown in Figure 4, where we plot the measured Li EW's (corrected for the contribution of the 6707.44 feature) as a function of  $(B-V)_o$ . The stars with a '?' radial velocity flag in Tab. 1 (apart from R53A which is a photometric nonmember) and R18 are marked in the figure; we first focus the discussion on these four objects. Li equivalent widths for R3 and R7 are within the range of values measured for cluster members at the same color and are therefore consistent with membership; in any case, their inclusion or exclusion from the sample would not change our conclusions. On the other hand, the EW for R80 is the lowest one measured among early-K dwarfs, though it is not greatly lower than for other objects of the same color; therefore, on one hand Li does not provide us with a definite criterion to decide about R80 membership; on the other hand, the inclusion of this star among members or non-members would put constraints on the range

of the Li dispersion for K dwarfs (see next section). Since this star was included in the original list of cluster members of Braes (1962), we decided to leave it in the sample and discuss it separately whenever necessary. R18 is an additional puzzling object: although both its photometry and radial velocity are consistent with it being an early-K dwarf cluster member, it does not show H $\alpha$  emission nor any Li and its Ca (6717.69 Å) EW is more typical of an F-type stars than of a K dwarf; Stauffer et al. (1997) indeed classify it as a nonmember. For this reasons we leave this object out of our sample.

Fig. 4 does not show a tight Li vs. color relationship. A star-to-star scatter in Li EW's of the order of 100 mÅ is present among late-G and early-K stars. A dispersion seems to be present also among earlier-G dwarfs, although narrower than for K dwarfs. The small number of objects in both the F and late-K/M spectral ranges does not allow us to establish whether a spread is present or not. However, the EW's of R7 and R79 ( $B-V=0.44$ ) and those of R21 and R85 ( $B-V\sim 0.5$ ), respectively, are in good agreement with each other, suggesting that probably

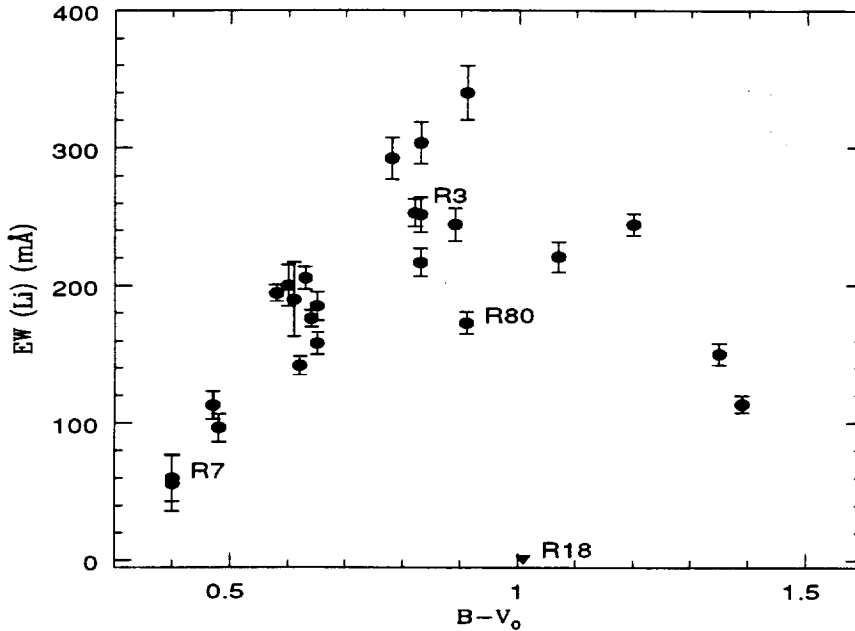


Fig. 4. Measured EW's of the Li doublet (in mÅ) corrected for the contribution of the 6707.44 Fe I line vs. dereddened B-V. Uncertain cluster members are marked.

F stars in IC 2602 are not affected by any major dispersion in Li.

In order to ascertain whether observational uncertainties could account for the dispersion in EW's among later-type stars, we plot in Figure 5a Li EW's as a function of  $(B-V)_o$ , considering only objects in the  $0.5 \leq (B-V)_o \leq 1$  range. In Figure 5b Ca I 6717.69 Å EW's are plotted as a function of  $(B-V)_o$  for the same objects. The comparison between the two figures indicates that the scatter in Li EW's exceeds, at each color, the scatter in Ca 6717.69 Å EW's. More quantitatively, if we consider the four objects with  $(B-V)_o \sim 0.83$  (i.e., R3, R14, R68, R95) and compute the standard deviation from the mean for the Li and Ca equivalent widths ( $\sigma_{Ca}$  and  $\sigma_{Li}$ ), we obtain  $\sim 36$  and  $\sim 14$  mÅ, respectively. At earlier-types, if we consider the five objects with  $(B-V)_o$  around 0.65 (R35, R45, R66, R70 and R92), we get  $\sigma_{Ca} \simeq 9$  mÅ and  $\sigma_{Li} \simeq 24$  mÅ. Since the strength of the Ca feature is a function of color, the dispersion in Ca equivalent widths gives an additional estimate of the observational uncertainties indicating that the dispersion in Li equivalent widths is larger than what is expected from errors in EW's measurements.

#### 4.1.2. Abundances

In Figure 6a we plot the  $\log n(Li)_{LTE}$  abundances as a function of effective temperature, while in Fig. 6b NLTE abundances are shown (for stars with  $T_{eff} < 4500$  K, for which NLTE abundances were not available, LTE abundances are used). The two lines delimit the range of the initial Li content for Pop. I stars, as indicated by pre-main sequence stars (both Classical and Weak T Tauri stars; e.g., Magazzù et al. 1992; Martín et al. 1994) and meteorites. Fig. 6a illustrates the usual pattern of decreasing Li with decreasing temperature, which is observed in older clusters; the coolest objects in the sample show indeed a rather low Li content, indicating that at 30 Myr a significant depletion has already occurred among low mass stars. The star-to-star scatter in Li EW's reflects into a scatter in  $\log n(Li)$ . The maximum  $\log n(Li)$  among IC 2602 members is generally consistent with the primordial value, although two of the most Li-rich G dwarfs (R72 and R83) have apparently a slightly higher Li (about 0.15 dex). Fig. 6b, however, shows that abundances higher than 3.2–3.3 are most likely due to neglecting NLTE effects; NLTE abundances for R72 and R83 are indeed in agree-



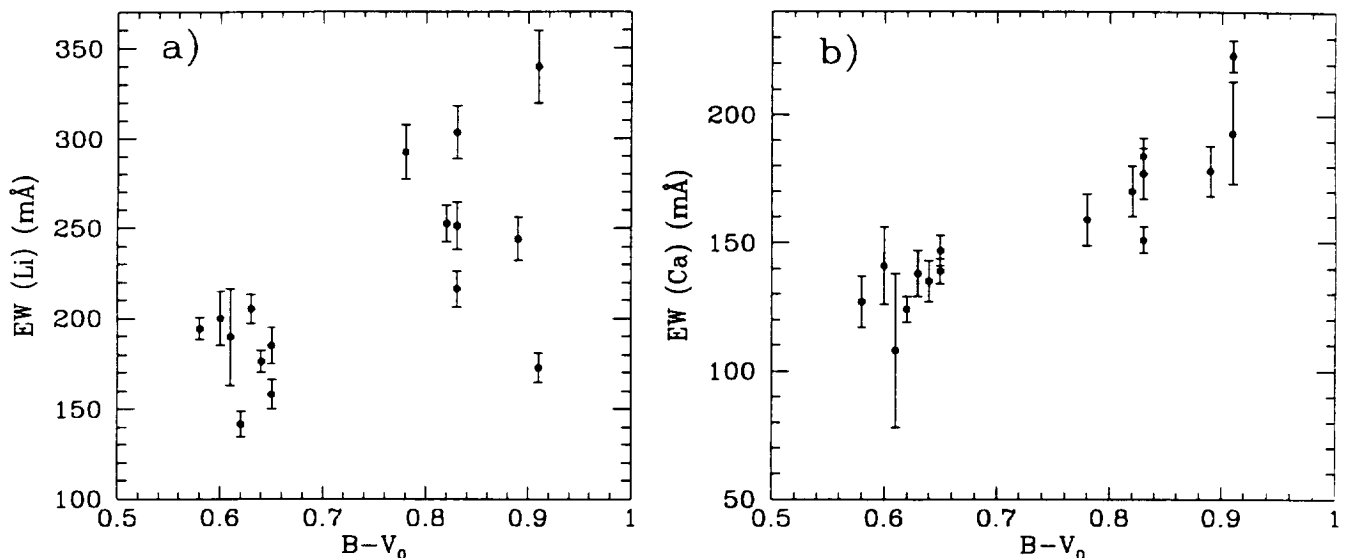


Fig. 5. a) Same as Fig. 4, but only stars with  $0.5 < (B-V)_0 < 1$  are plotted; b) Ca 6717.69 Å EW's as a function of  $(B-V)_0$  for the same stars as in panel a).

ment with the primordial value. More generally, NLTE corrections result in lower abundances, with the difference  $\log n(\text{Li})_{NLTE} - \log n(\text{Li})_{LTE}$  increasing with decreasing  $T_{eff}$  and increasing  $\log n(\text{Li})$ , i.e. NLTE effects become more important as the Li line gets stronger (see discussion in Carlsson et al.). As a consequence, NLTE corrections for Li-rich dwarfs are larger than for Li-poor ones, so that the range of dispersion appears partly reduced (though not completely eliminated!) We believe that NLTE values for the lithium abundance are likely to be more correct both because this is in principle a better treatment of the physics, and because we regard it as unlikely that some of our G-type stars have abundances larger than the initial Pop. I value, while the F dwarfs show Li abundances consistent with the primordial value.

#### 4.2. Comparison with other clusters

In Figure 7 we compare  $\log n(\text{Li})$  vs.  $T_{eff}$  for IC 2602 with the Pleiades (Soderblom et al. 1993a, García Lopez et al. 1994) and  $\alpha$  Per (Balachandran et al. 1988, 1996). Li abundances for the Soderblom et al.'s sample were corrected for NLTE effects using Carlsson et al.'s code. Both temperatures and abundances for  $\alpha$  Per stars and García Lopez et al.'s Pleiades were recomputed using the published EW's, but using the same  $T_{eff}$  vs.  $B-V$  calibration, COG's, and NLTE corrections as for IC 2602. Fig. 7 indicates that the IC 2602 datapoints generally lie on the upper envelope of the  $\log n(\text{Li}) - T_{eff}$  pattern for the Pleiades. Warm stars (with  $T_{eff} > 6200$  K) in the three clusters seem to have, on average, the same  $\log n(\text{Li})$ , which is also the initial content for Pop. I stars. As we move towards cooler temperatures, Pleiades,  $\alpha$  Per, and a few IC 2602 stars begin to show signs of Li

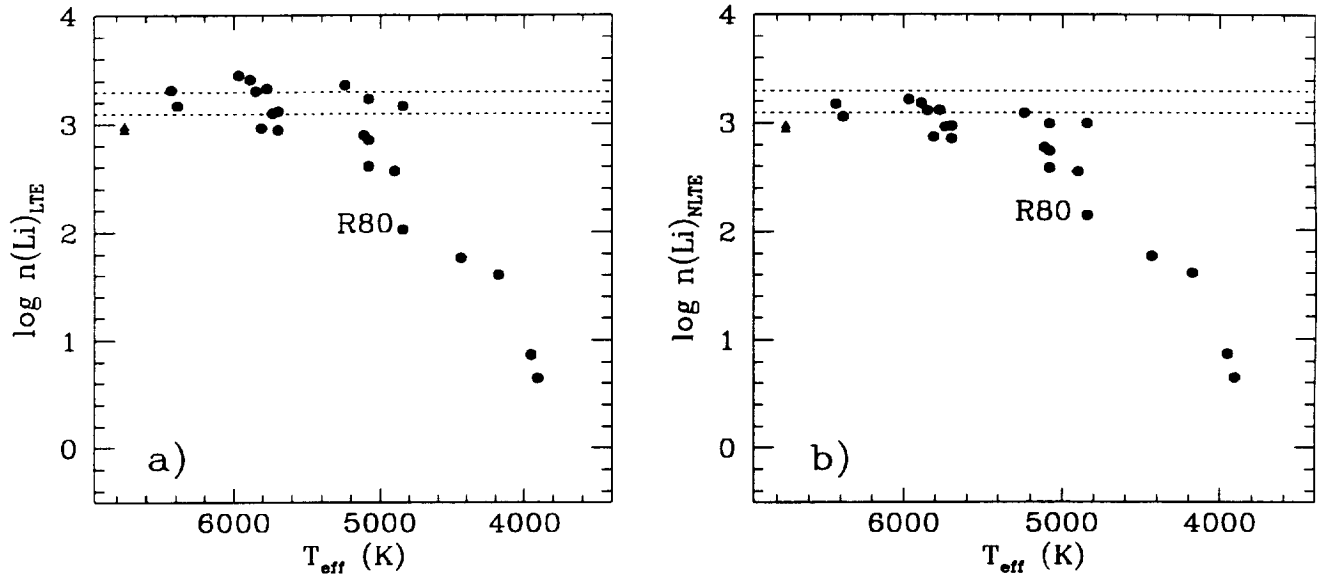


Fig. 6. a) LTE Li abundances as a function of effective temperature for our sample stars; b) Same as in panel a), but NLTE Li abundances are shown. For stars cooler than 4500 K LTE abundances are plotted.

depletion, while the remaining IC 2602 objects in the same temperature range still retain their initial Li. As to late-G and early-K objects, the *maximum* abundance in the three clusters is comparable and somewhat lower than the initial content. On the other hand, the lowest abundance among IC 2602 stars with  $T_{eff} \sim 5000$  K, is significantly higher than for the Pleiades, and thus a smaller dispersion is observed. Finally, three of the four objects in the late-K/early-M spectral range lie above all of the Pleiades and  $\alpha$  Per members of that color, whereas the fourth one lies within the range occupied by the members of the two other clusters.

Given the different evolutionary status of the three clusters and the different PMS turn-on points, we are not comparing stars with the same mass, when we compare Pleiades,  $\alpha$  Per and IC 2602 late-type stars at the same temperature. Specifically, IC 2602 stars cooler than  $\sim 5600$  K are more massive than Pleiades and  $\alpha$  Per stars of the

same temperature, with the difference increasing with decreasing  $T_{eff}$ . This is shown in Figure 8, where the  $\log T_{eff}$  vs.  $\log M/M_{\odot}$  isochrones at 30, 50 and 70 Myr are plotted. In the figure D'Antona & Mazzitelli (1994) PMS evolutionary tracks which employ Canuto & Mazzitelli (1990, 1992) turbulent convection treatment and Alexander et al. (1989) and Roger & Iglesias (1992) opacities are shown. We determined masses for our sample stars, the Pleiades, and  $\alpha$  Per using the mass- $T_{eff}$  isochrones shown in Fig. 8. In Figure 9 Li abundances are plotted as a function of  $\log M/M_{\odot}$  for IC 2602, the Pleiades, and  $\alpha$  Per. The figure shows that for solar-type stars the distribution of IC 2602 points with respect to the Pleiades and  $\alpha$  Per is not very dissimilar from that of Fig. 7. Although our sample includes only eight stars with masses  $1M_{\odot} \pm 0.1$ , and thus we cannot draw any definitive conclusion, the figure indicates that stars slightly more massive than the Sun in IC 2602 have retained their initial Li, while Pleiades and

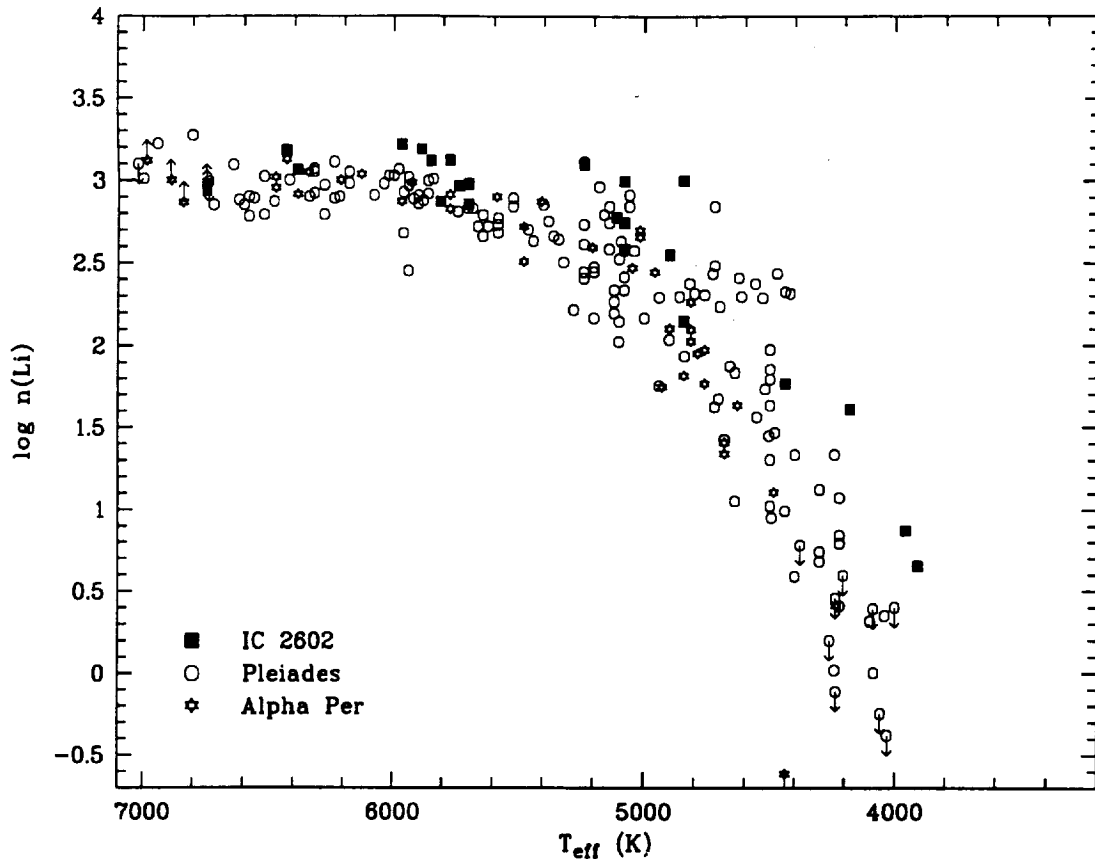


Fig. 7. NLTE Li abundances vs. effective temperature for IC 2602 stars (filled squares), the Pleiades (open circles), and  $\alpha$  Per (stars).

$\alpha$  Per members with similar masses have undergone some depletion; this suggests that MS Li burning is efficient at  $\sim 1M_{\odot}$  from the very earliest phases on the ZAMS. A few IC 2602 stars as massive as the Sun, or with slightly lower masses, show some Li depletion. Solar-type stars at 30 Myr have just arrived on the ZAMS: the PMS turn-on point is at  $\sim 1M_{\odot}$ , while in the Pleiades it is at about  $0.7\text{--}0.6 M_{\odot}$  (see Figs. 5a and 5b in Stauffer et al. 1997): the observed Li content of these IC 2602 stars should be the result of PMS processes only. The  $\log n(\text{Li})$  vs. mass pattern in Fig. 9 therefore suggests that PMS Li destruction starts to occur at about  $1M_{\odot}$ , but with an efficiency which varies from star to star, causing a slight dispersion in  $n(\text{Li})$ . This small dispersion has basically disappeared by the age of the Pleiades. As to very low mass stars, the distribution in Fig. 9 appears reversed with respect to that of Fig. 7: the four IC 2602 stars with masses lower than  $0.8 M_{\odot}$  have  $\log n(\text{Li})$  as low as that of the most Li depleted Pleiades objects at the same mass. The first question one should ask is whether this is a *real* effect or it is rather due to the use of an inaccurate mass vs.  $T_{\text{eff}}$  relationship. Determining masses from effective temperatures is indeed somewhat

critical. D'Antona & Mazzitelli pointed out that the location of their tracks on the HR diagram (and hence the  $T_{\text{eff}}$  - mass relationship) is model dependent, in particular for  $M \leq 0.6M_{\odot}$ . We generated plots similar to the one shown in Fig. 9, but using masses determined by employing different evolutionary models (namely, D'Antona & Mazzitelli's models 2 and 3, and Pinsonneault et al.'s model (1990)). These plots are shown in Figures 10a.b.c. In the figures only Pleiades and IC 2602 are plotted.

Fig. 10 indicates that the relative positions of the IC 2602 and the Pleiades datapoints in the  $\log n(\text{Li})$  vs. mass diagram are somewhat affected by the choice of the model, in particular for low mass stars. However, in none of these plots do the four lowest mass IC 2602 objects lie above the Pleiades as was the case in the  $\log n(\text{Li})$  vs.  $T_{\text{eff}}$  diagram. We conclude that, given both the uncertainties and the small IC 2602 sample size, such low abundances are not completely inconsistent with the results for the Pleiades: nevertheless, the presence of these four stars showing a depletion that is at least similar to that of the older Pleiades, suggests that either PMS destruction in low mass dwarfs stops working between 30 and 70 Myr, or that the Pleiades

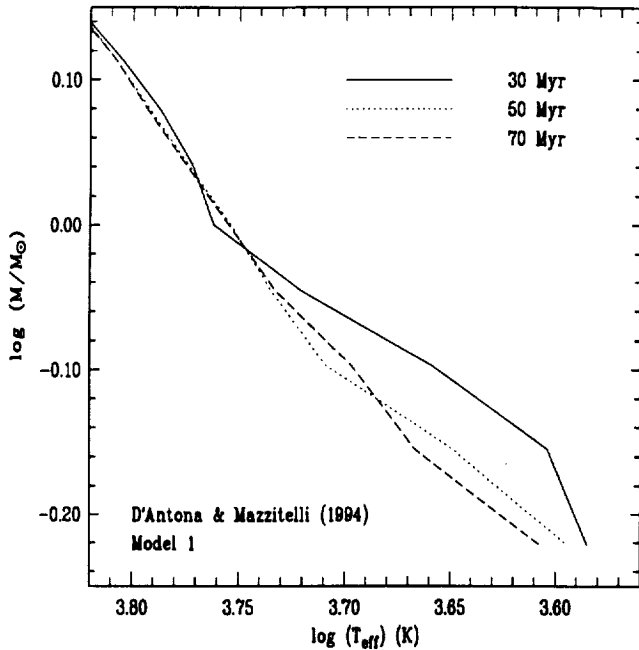


Fig. 8. Mass-temperature isochrones for 30 Myr (solid line), 50 Myr (dotted line) and 70 Myr (dashed line). D'Antona & Mazzitelli (1994) model 1 was adopted.

stars have undergone less PMS depletion than their IC 2602 counterparts. A third possibility is that either the age of the Pleiades or those of  $\alpha$  Per and IC 2602 are largely in error, or that the clusters are characterized by a large spread in age. This is regarded as very unlikely by both Soderblom et al. (1993a) for the Pleiades and Stauffer et al. (1997) for IC 2602. Note that if the age scale were wrong, it would be difficult to explain why solar-type stars in IC 2602 lie above the Pleiades.

#### 4.3. Comparison with theoretical models

In Figures 11a and 11b the  $\log n(\text{Li})$  vs. mass distributions for the Pleiades and IC 2602 are compared with different theoretical predictions. Specifically, the three curves in Fig. 11a represent three different PMS models from D'Antona & Mazzitelli (1994), who consider the standard convective mixing and nuclear burning as the only Li destruction mechanism in the PMS phase. The three curves correspond to the models for 30 Myr; however, all D'Antona & Mazzitelli models predict no significant difference in Li depletion between 30 and 70 Myr. Fig. 11b shows the theoretical predictions of Pinsonneault et al.'s (1990) models which take into account stellar rotation as an additional parameter, and mixing of material due to angular momentum transport. According to these models, different initial angular momenta result in both different surface rotational velocities and different Li abundances. The two figures show that all the models predict no PMS destruction for stars with  $M > 1.25M_{\odot}$ , in agreement with

observations. On the contrary, all the models predict too much Li destruction for lower masses. In particular, D'Antona & Mazzitelli model 1 is clearly discrepant with the measured abundances already for solar-type stars; D'Antona & Mazzitelli models 2 and 3 give a better fit of the lower envelope of the  $\log n(\text{Li})$  vs. mass distribution, but fail to reproduce the abundances of very low mass stars. All three models do not predict basically any difference in abundance between the Pleiades and IC 2602, which is also at variance with the observational results. Finally, since their models depend only on stellar mass, they are unable to reproduce the observed dispersion. On the contrary, Fig. 11b indicates that assuming a range of initial angular momenta would allow a range in  $\log n(\text{Li})$ , with the dispersion in  $\log n(\text{Li})$  increasing with decreasing mass, which is what we observe. However, even the model with the smallest  $J_0$  results in too high a Li destruction (particularly among solar-type stars). Moreover, the models do not predict any difference between the Pleiades and IC 2602 for solar mass stars, whereas they predict that, for a given  $J_0$ , Pleiades low mass stars should be more depleted than IC 2602 stars. We conclude that, while Pinsonneault et al.'s models could qualitatively explain the star-to-star scatter (at least among low mass stars) in a given cluster, they fail to reproduce both the total amount of Li depletion and the cluster to cluster differences.

As a final remark, we note that D'Antona & Mazzitelli (1994) and Pinsonneault et al. (1990) both adopted a solar metallicity in their models. However D'Antona

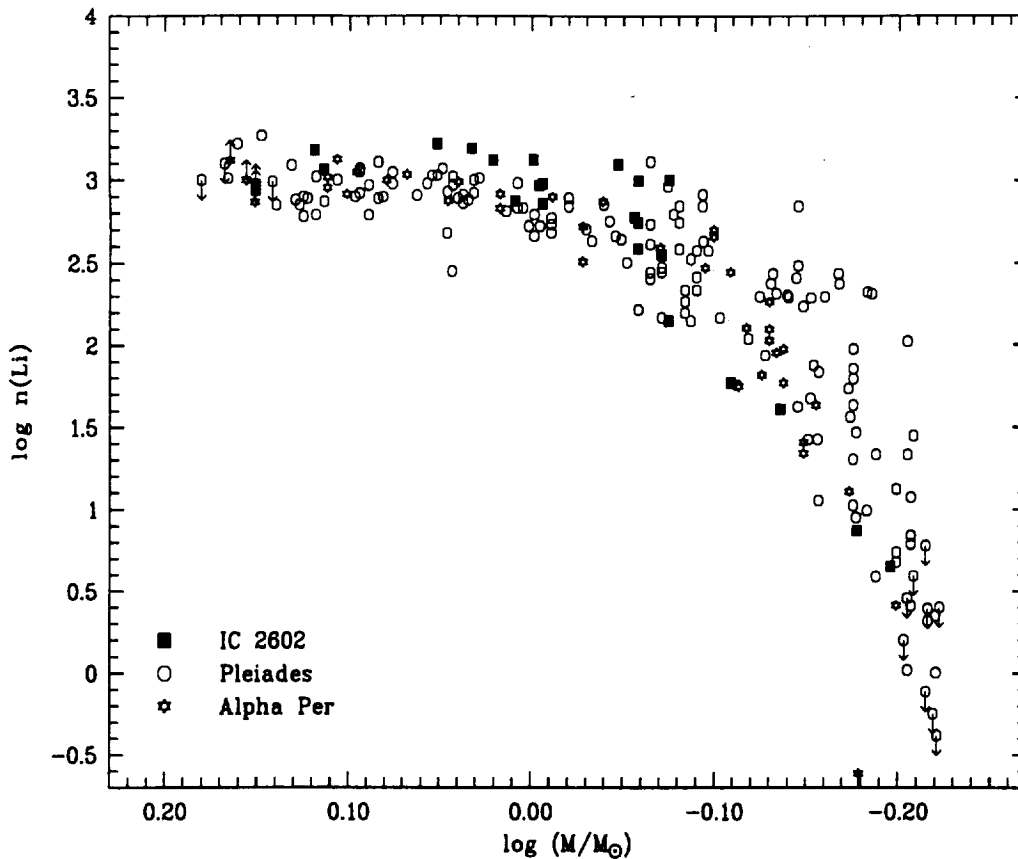


Fig. 9. Same as in Fig. 7, but Li abundances are plotted as a function of the logarithm of the mass. Masses for stars in the three clusters have been derived using the mass- $T_{eff}$  relationships shown in Fig. 8.

& Mazzitelli (1994), referring to D'Antona & Mazzitelli (1984) and to Deliyannis & Demarque (1991), pointed out that the amount of PMS Li depletion is strongly influenced by the assumed metallicity. Lower metallicity results in a lower Li destruction rate. Although they were mainly interested in explaining the Li vs.  $T_{eff}$  pattern for the Hyades, Swenson et al. (1994a,b) have also shown that metallicity and, more in general, abundances of other heavy elements (Oxygen in particular), affect stellar opacities and PMS Li destruction. According to D'Antona & Mazzitelli (1984) for a  $0.7 M_{\odot}$  the  $Z=0.02$  model predicts a factor of  $\sim 20$  higher Li destruction than the  $Z=0.001$  model, whereas for  $0.9 M_{\odot}$  the higher metallicity models predicts only a factor  $\sim 1.5$  higher depletion. This indicates that even a small difference in metallicity between the Pleiades and IC 2602 could cause a significant difference in Li PMS destruction among low mass dwarfs, without affecting solar-type stars. Iron abundances for 12 Pleiades dwarfs have been determined by Boesgaard & Friel (1990), giving an average metallicity  $[Fe/H] = -0.034$ . The determination of metallicity for IC 2602 will help resolve this issue.

#### 4.4. Lithium and rotation

Both Soderblom et al. (1993a) and García Lopez et al. (1994) have pointed out that stellar rotation plays a fundamental role in Li destruction/preservation at least as far as stars in the  $\sim 5500$ – $4500$  K temperature range are concerned. An initial dispersion in rotational parameters, i.e. either angular momenta or surface rotational velocities, is therefore the most likely cause of the dispersion in Li, as Pinsonneault et al.'s models discussed in the previous section also indicate.

So far we have not discussed in detail rotational velocities for IC 2602 candidates, and in particular the possible presence of a relationship between  $v \sin i$  and Li. Figure 12 is the same as Fig. 6b, but stars with different rotational velocities are represented by symbols of different sizes. The Li-rotation relationship in Fig. 12 is not as evident as for the Pleiades, particularly among warmer stars. Nevertheless, if we look at the  $\sim 5400$ – $4800$  K  $T_{eff}$  interval, the most Li-rich stars are generally the most rapidly rotating ones. The only exception is R95A; the low  $v \sin i$  of this stars, however, may be due to projection effect since both its X-ray luminosity ( $\log L_X = 30.28$ , see Randich et al.

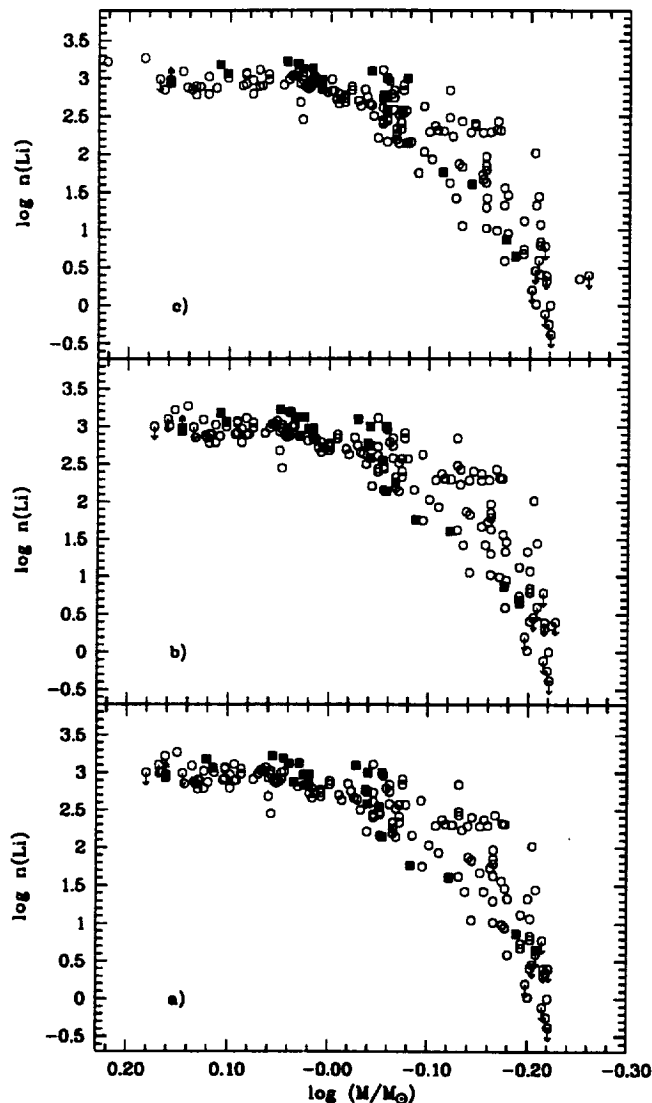


Fig. 10. Same as Fig. 9, but using masses determined using different evolutionary tracks. Namely, a) D'Antona & Mazzitelli's model 2 was used; b) D'Antona & Mazzitelli's model 3 was used; c) Pinsonneault et al.'s model was used. Only IC 2602 (filled squares) and the Pleiades (open circles) are plotted.

1995) and its  $H\alpha$  EW indicate a high level of activity. To conclude, we think that our data suggest a Li-rotation link, at least among late-G/early-K stars, indicating that such a link may indeed develop during the PMS phases.

Martín & Claret (1996) have recently suggested that there may indeed be a physical basis for a link between high rotation and reduced Li destruction. They computed

PMS rotating models for  $0.8-0.7 M_{\odot}$  stars and found that the temperature at the base of the convective zone is lower in rotating models; convective mixing therefore does not lead as readily to Li destruction and rapid rotators in this mass range would be predicted to be more Li rich.

We also note that the rotational velocity distribution of solar type stars in IC 2602 is characterized by a larger dis-

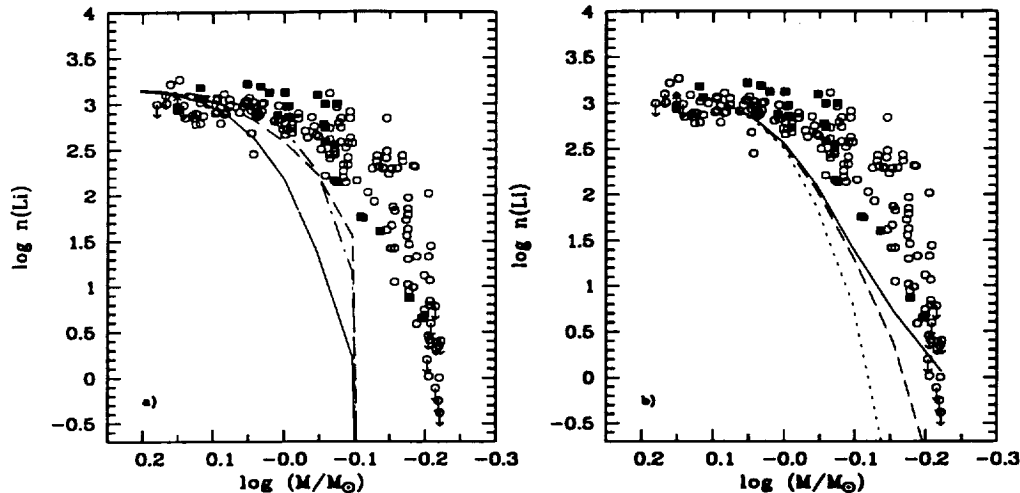


Fig. 11. Comparison of the  $n(\text{Li})$  vs. mass distribution for IC 2602 stars (filled squares) and the Pleiades (open circles) with theoretical predictions. Specifically, in panel a) D'Antona & Mazzitelli (1994) 30 Myr models are shown. The solid line corresponds to the model with Canuto & Mazzitelli convection treatment and Alexander + Rogers & Iglesias opacities (their Table 1); the dashed line indicates the model with the same convection treatment, but Kurucz (1991) opacities (their Table 2), while the dash-dotted curve denotes the model with the Alexander + Rogers & Iglesias opacities, but using the mixing length theory prescription for convection (their Table 3). In panel b) Pinsonneault et al.'s (1990) models are plotted. The solid and dashed lines represent the 30 Myr model computed with two different values of the initial angular momentum  $J_0$  ( $\log J_0 = 49.2$  and  $50.2$ , where  $J_0$  has units of  $\text{g cm}^2 \text{s}^{-1}$ ). The dotted curve denotes the  $\log J_0 = 49.2$  model at 70 Myr.

persion and by typically larger maximum velocities than their Pleiades counterparts (Stauffer et al. 1997), which have already undergone some MS spin-down. This coincides with the fact that Pleiades G dwarfs show both less Li than their IC 2602 counterparts and basically no star-to-star-scatter. The same convergence in Li and rotation occurs when comparing K dwarfs in the Pleiades and the Hyades, suggesting that MS spin-down, and possibly transport of angular momentum as a mixing mechanism, tend to wash out the initial (i.e., upon arrival on the ZAMS) spread in both  $v \sin i$  and lithium.

## 5. Conclusions

We have presented Li observations of a sample of solar-type and low mass dwarfs in the 30 Myr old cluster IC 2602. Our observations have allowed us to answer one

of the questions raised by Soderblom et al. (1993a), i.e., when does the dispersion in Li develop? We have shown that the spread among late-G/early-K dwarfs develops in the PMS phase. Moreover, there is an indication that, at younger ages, a small star-to-star scatter is present also among early-G stars.

The comparison with the Pleiades and  $\alpha$  Per shows that PMS Li destruction starts to be efficient at around  $1 M_\odot$ . Surprisingly, we find that the latest-type stars in IC 2602 do not have higher Li than the Pleiades, as one would expect given the difference in age between the two clusters. If confirmed, the higher Li depletion of late-type stars in IC 2602 could be explained by a difference in metallicity between the two clusters. We need a larger sample to confirm whether this is a general feature, or whether stars more Li-rich than the most Li rich Pleiades are also present in IC 2602. A larger sample will allow us to de-

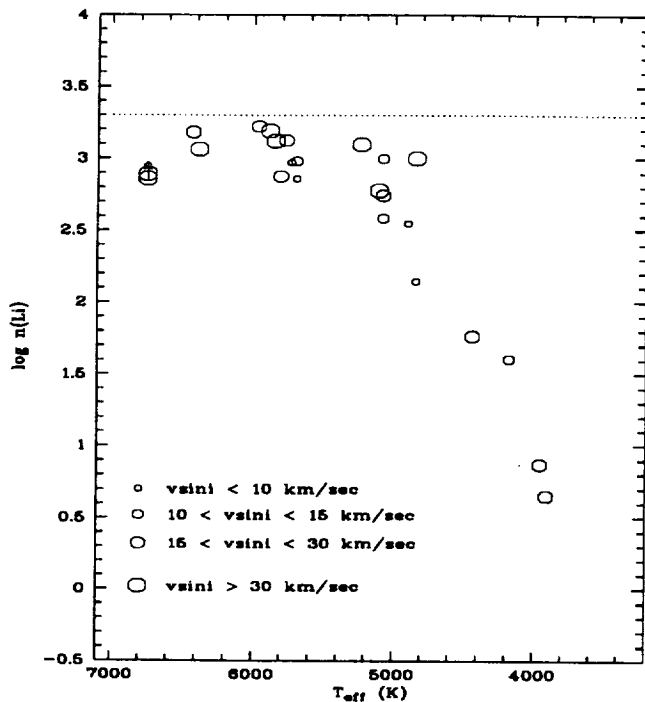


Fig. 12. Same as in Fig. 6b, but stars in different rotational velocity bins are indicated by symbols of increasing size.

termine whether a spread in Li is present also among very late-type stars.

*Acknowledgements.* SR acknowledges Luca Pasquini for useful discussions. JS acknowledges support from NASA Grant NAGW-2698.

## References

- Abt, H.A., and Morgan, W.W. 1972, ApJ 174, L131  
 Alexander, D.R., Augason, G.C., and Johnson, H.R. 1989, ApJ 345, 1014  
 Arribas, S., and Roger, C. 1989, A&A 215, 305  
 Balachandran, S. 1995, ApJ 446, 203  
 Balachandran, S., Lambert, D.L., and Stauffer, J.R. 1988, ApJ 333, 267  
 Balachandran, S., Lambert, D.L., and Stauffer, J.R. 1996, ApJ erratum, submitted  
 Barnes, S., and Sofia, S. 1996, ApJ 462, 746  
 Bessel, M.S. 1979, PASP 91, 589  
 Boesgaard, A.M., and Tripicco, M.J. 1986, ApJ 303, 724  
 Boesgaard, A.M., and Friel, E.D. 1990, ApJ 351, 467  
 Boesgaard, A.M., Budge, K.G., and Ramsay, M.E. 1988, ApJ 327, 389  
 Bouvier J. 1996, A&AS 120,127  
 Braes, M.S. 1962, Bull. Astron. Inst. Neth. 16, 297  
 Butler, R.P., Cohen, R.D., Duncan, D.K., and Marcy, G.W. 1987, ApJ 351,467  
 Campbell, B. 1984, ApJ 283, 209  
 Canuto, V.M., and Mazzitelli, I. 1990, ApJ 370, 295  
 Canuto, V.M., and Mazzitelli, I. 1992, ApJ 389, 724  
 Carlsson, M., Rutten, R., Bruls, J.H.M.J., and Schukina, N.G.. 1994, A&A 288, 860  
 D'Antona, F., and Mazzitelli I. 1984, A&A 138, 431  
 D'Antona, F., and Mazzitelli I. 1994, ApJS 90, 467  
 Deliyannis, C.P., and Demarque, P. 1991, ApJ 379, 216  
 Duncan, D.K., and Jones, B.F. 1983, ApJ 271, 663  
 García Lopez, R., Rebolo, R., Magazzù A., and Beckman, J.E. 1991, MSAIt 62, 187  
 García Lopez, R.J., Rebolo, R., and Martín, E.L. 1994, A&A 282, 518  
 Kurucz, R.L. 1991, in *Stellar Atmospheres: Beyond the Classical Models*, ed. L. Crivellari, I. Hubeny, and D.G. Hummer. 441  
 Magazzù, A., Rebolo, R., and Pavlenko, Ya. V 1992, ApJ 392, 159  
 Martín, E.L., Rebolo, R., Magazzù, A., and Pavlenko, Ya. V. 1994, A&A 282, 503  
 Martín, E.L., and Claret, A. 1996, A&A 306, 408  
 Michaud, G., and Charbonneau, P. 1991, SSRv 57, 1  
 Pasquini, L. 1993, Update to the ESO operating manual #2  
 Pasquini, L., Liu, Q., and Pallavicini, R. 1994, A&A 287, 191  
 Pasquini, L., Randich, S., and Pallavicini, R. 1997, in preparation  
 Pinsonneault, M.H., Kawaler, S.D., and Demarque, P. 1990, ApJS 74, 501  
 Pinsonneault, M.H., Kawaler, S.D., Sofia, S., and Demarque, P. 1989, ApJ 338, 424  
 Prosser, C.F., Randich, S., and Stauffer, J.R. 1996, AJ 112, 649  
 Randich, S., Schmitt, J.H.M.M., Prosser, C.F., and Stauffer, J.R. 1995, A&A 300, 134  
 Rogers, F.J., and Iglesias, C.A. 1992, APJS 79, 507  
 Soderblom, D.R. 1989, ApJ 342, 823  
 Soderblom, D.R. 1995, in 'The Light Element Abundances', P. Crane ed., p. 272  
 Soderblom, D.R., Oey, M.S., Johnson, D.R.H., and Stone,, R.P.S. 1990, AJ 99, 595  
 Soderblom, D.R., Jones, B.F., Balachandran, S., et al 1993a, AJ 106, 1059  
 Soderblom, D.R., Stauffer, J.R., Hudon, J.D., and Jones, B.F. 1993b, ApJS 85, 315  
 Soderblom, D.R., Jones, B.F., Stauffer, J.R., and Chaboyer, B.C. 1995, AJ 119, 729  
 Stauffer, J.R., Hartmann, L.W., Prosser, C.F., Randich, S., Balachandran, S., et al. 1997, ApJ, in press  
 Swenson, F.J., Faulkner, J., Iglesias, C.A., Rogers, F.J., and Alexander, D.R. 1994a, ApJ 422, L79  
 Swenson, F.J., Faulkner, J., Rogers, F.J., and Iglesias, C.A. 1994b, ApJ 425, 286  
 Thorburn, J.A., Hobbs, L.M., Deliyannis, C., and Pinsonneault, M.H. 1993, ApJ 415, 150  
 Whiteoak, J.B. 1961, MNRAS 123, 245